

Reactivities of Isomerization, Oxidation, and Dimerization of Radical Cations of Stilbene Derivatives

Tetsuro Majima,^{*,†} Sachiko Tojo, Akito Ishida, and Setsuo Takamuku*

The Institute of Scientific and Industrial Research, Osaka University, Mihogaoka 8-1, Ibaraki, Osaka 567, Japan

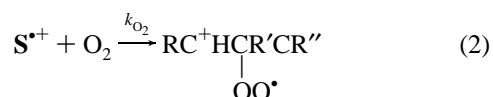
Received: April 2, 1996[⊗]

Reactions of radical cations of eight stilbene derivatives ($S^{\bullet+}$) have been studied using pulse radiolysis and γ -ray radiolysis in 1,2-dichloroethane or butyl chloride. Unimolecular isomerization from *cis*- $S^{\bullet+}$ to *trans*- $S^{\bullet+}$ and bimolecular reactions with O_2 (oxidation) and a neutral stilbene (dimerization) occur depending on the substituents. The unimolecular *c*-*t* isomerization and the oxidation proceed preferably in $S^{\bullet+}$ substituted with a *p*-methoxyl group (as an electron-donating substituent) with rate constants of $k_i = 4.5 \times 10^6$ to 1.4×10^7 s^{-1} and $k_{O_2} = (1.2-4.5) \times 10^7$ $M^{-1} s^{-1}$, respectively. On the basis of transient absorption measurements, it is concluded that separation and localization of a positive charge and an unpaired electron play the most important role as the controlling factors in the reactivities of the unimolecular isomerization and the oxidation. The dimerization involves initial formation of a π -complex with overlapping of two benzene rings and is inhibited by steric hindrance of substituents on the benzene rings and olefinic carbons.

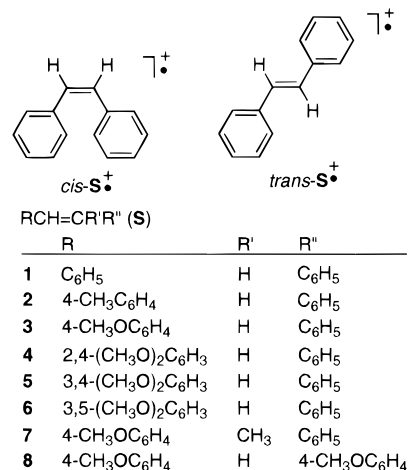
Introduction

It is well-known that *cis*(*c*)-*trans*(*t*) isomerization, dimerization, and addition of a nucleophile occur in radical cations of aromatic olefins as typical reactions.¹⁻⁵ The reactivities depend on the structure or substituents of the radical cations. However, a rather small number of the rate constants for the reactions have been reported despite numerous studies from synthetic and mechanistic points of view.¹⁻⁵ Therefore, factors that control the reactivities of the radical cations are still unclear. Even those of the stilbene radical cation ($St^{\bullet+}$) are not completely established.²⁻⁴ No unimolecular *c*-*t* isomerization occurs in $St^{\bullet+}$,² although it does in the radical cations of *c*-4,4'-dibromostilbene and *c*-4,4'-dimethylstilbene.^{2c} Dimerization³ of $St^{\bullet+}$ with *St* occurs with a rate constant of $k_d = (3.5-3.9) \times 10^8$ $M^{-1} s^{-1}$ ^{3c,d} to yield a π -dimer radical cation (π - $St_2^{\bullet+}$) with overlapping π -electrons between the two benzene rings, which converts to a σ -dimer radical cation (σ - $St_2^{\bullet+}$) with an acyclic linear structure having both a radical and a cation on the 1- and 4-positions of the C_4 linkage, decomposing to *t*- $St^{\bullet+}$ and *St* as final products.^{3d} It is reported that *t*- $St^{\bullet+}$ reacts with a superoxide molecule^{4a-e} at a rate constant of $k_{SO} = 1.9 \times 10^9$ $M^{-1} s^{-1}$ near the diffusion rate constant,^{4e} while *t*- $St^{\bullet+}$ has little reactivity toward O_2 .^{3a,4,5} On the other hand, a high reactivity of $k_{O_2} = 2.6 \times 10^8$ $M^{-1} s^{-1}$ has been reported for the radical cation of (*E*)-2,3-diphenyl-2-butene.^{4g}

In this article we wish to report three reactions of radical cations of eight stilbene derivatives ($S^{\bullet+} = RCH=CR'R'' = 1^{\bullet+}-8^{\bullet+}$) (Scheme 1) using pulse radiolysis and γ -ray radiolysis in 1,2-dichloroethane or butyl chloride,⁶ unimolecular isomerization from *cis* to *trans* isomer radical cations (eq 1), and bimolecular reactions with O_2 (oxidation, eq 2) and a neutral stilbene (dimerization, eq 3).



SCHEME 1



On the basis of the rate constants of the three types of reactions, we have found that the unimolecular *c*-*t* isomerization and oxidation with O_2 of radical cations of stilbene derivatives, particularly with substitution of a *p*-methoxyl group as an electron-donating substituent in the $S^{\bullet+}$ derivatives, enhance remarkably the isomerization and oxidation at room temperature. It is concluded that separation and localization of a positive charge and an unpaired electron play the most important role in increasing the reactivities.⁶

Experimental Section

General. Pulse radiolyses were performed, as described previously,^{3d} using an electron pulse (28 MeV, 8 ns, 0.7 kGy per pulse) from a linear accelerator at Osaka University. The temperature was controlled by circulating thermostated aqueous ethanol around the quartz sample cell. γ -Radiolysis of 1,2-dichloroethane (DCE) solutions or butyl chloride solutions at a concentration of 1.0×10^{-2} M was carried out in a Pyrex tube with an inner diameter of 1.0 cm or in 1.5-mm-thick Suprasil cells at 77 K for UV-vis absorption measurements, respectively, using a ⁶⁰Co γ source (dose, 2.6×10^2 Gy).^{3d} Optical absorption spectra were taken by a spectrophotometer and a multichannel photodetector.

The **S**-containing solutions for spectral measurements at 77 K were degassed by freeze-pump-thaw cycles, while those

[†] Tel: Japan+6-879-8496; FAX: Japan+6-875-4156; e-mail: majima@sanken.osaka-u.ac.jp.

[⊗] Abstract published in *Advance ACS Abstracts*, July 15, 1996.

TABLE 1: Transient Absorption Peaks (λ_{\max}) and the Molar Absorption Coefficients at the Peak (ϵ_{λ}) of D_1 and D_2 of $c\text{-S}^+$ and $t\text{-S}^+$ ($S^+ = 1^+ - 11^+$) Obtained by Pulse Radiolyses of c - and t -S ($S = 1 - 11$) (5.0×10^{-3} M) in DCE at Room Temperature^a

S^+	RCH=CR'R''			λ_{\max}/nm ($\epsilon_{\lambda}/\text{M}^{-1} \text{cm}^{-1}$)			
	R	R'	R''	D_2 of $c\text{-S}^+$	D_2 of $t\text{-S}^+$	D_1 of $c\text{-S}^+$	D_1 of $t\text{-S}^+$
1^+	Ph	H	Ph	515 (18 000)	480 (65 000)	780 (6180)	750 (11 400)
2^+	4- $\text{CH}_3\text{C}_6\text{H}_4$	H	Ph	520 (30 900)	490 (80 900)	780 (11 500)	790 (19 600)
3^+	4- $\text{CH}_3\text{OC}_6\text{H}_4$	H	Ph	530 (13 200)	470, 500 (39 200, 74 800)	nd	720, 800 (14 700, 41 700)
4^+	2,4- $(\text{CH}_3\text{O})_2\text{C}_6\text{H}_3$	H	Ph	530 (nd)	480 (105 000)	nd	680 (14 700)
5^+	3,4- $(\text{CH}_3\text{O})_2\text{C}_6\text{H}_3$	H	Ph	540 (nd)	480 (84 600)	nd	700 (14 700)
6^+	3,5- $(\text{CH}_3\text{O})_2\text{C}_6\text{H}_3$	H	Ph	520 (3270)	460, 510 (24 500, 20 800)	700 (1240)	>900 (>11 000)
7^+	4- $\text{CH}_3\text{OC}_6\text{H}_4$	CH_3	Ph	450, 500 (8820, 9710)	440, 490 (18 400, 29 400)	760, 780 (7940, 7940)	740, 800 (9810, 184 000)
8^+	4- $\text{CH}_3\text{OC}_6\text{H}_4$	H	4- $\text{CH}_3\text{OC}_6\text{H}_4$	nd	480, 540 (33 100, 76 000)	nd	780, 880 (24 500, 61 300)
9^+	4- $\text{CH}_3\text{OC}_6\text{H}_4$	$(\text{CH}_2)_3$	4- $\text{CH}_3\text{OC}_6\text{H}_4$	490, 560 (40 000, 16 000)		790, >850 (13 000, 20 000)	
11^+	4- $\text{CH}_3\text{C}_6\text{H}_4$	H	4- $\text{CH}_3\text{C}_6\text{H}_4$	500, 570 (20 000, 27 500)	nd	790, 900 (8130, >17 500)	nd

^a The molar absorption coefficients of ϵ_{λ} are estimated from the optical density at λ nm and the optical length of 1 cm with the assumption of a concentration of 8×10^{-6} M for S^+ , which is calculated from the optical density at 480 nm, the optical length of 1 cm, and $\epsilon_{480} = 6.5 \times 10^4 \text{ M}^{-1} \text{ cm}^{-1}$ for 1^+ in DCE.¹³

for pulse radiolyses were saturated by bubbling with Ar or O₂ for 20 min. Oxygen concentrations were varied by bubbling with a mixture gas of N₂ and O₂ premixed in a high-pressure cylinder at several ratios.

Half-wave oxidation potentials ($E_{p/2}^{\text{ox}}$) of 1.0×10^{-2} M samples were measured by cyclic voltametry using with a potentiostat and a function generator having a scan rate of 100 mV s⁻¹, a reference electrode of Ag/AgNO₃, a working electrode of a platinum disk, a pair electrode of platinum wire, and a supporting electrolyte of 10^{-1} M tetraethylammonium tetrafluoroborate in acetonitrile.

Materials. $c\text{-1}$ (Aldrich, 97%) and $t\text{-1}$ (>99.5%) were purchased from Aldrich and Tokyo Kasei and purified by means of distillation and recrystallization from ethanol, respectively, before use. The other stilbenes ($2\text{-}8$ and 11) were synthesized by the Wittig reaction of the corresponding substituted benzaldehyde and benzyltriphenylphosphonium chloride with sodium ethoxide in absolute ethanol at room temperature, according to literature procedures,⁷ and purified by means of distillation and column chromatography on silica gel and/or recrystallization from ethanol, respectively, before use. Analyses of the purified S by GC showed purities higher than 99.5%. 1,2-Bis(4-methoxyphenyl)cyclo-1-pentene (9) was prepared from the Grignard reaction of 2-chlorocyclopentanone and (4-methoxyphenyl)magnesium bromide, according to the literature,⁸ and was purified by recrystallization from methanol. Other chemicals were purchased from Tokyo Kasei and purified by distillation or recrystallization prior to use.

1,2-Dichloroethane (DCE) used as a solvent was distilled over calcium hydride. Butyl chloride was shaken with concentrated sulfuric acid, washed with water, dried over calcium chloride, and fractionally distilled.

Results

Formation and Reactions of S^+ ($S^+ = 1^+ - 8^+$). Formation and reactions of S^+ ($S^+ = 1^+ - 8^+$) were investigated using a pulse radiolysis technique in 1,2-dichloroethane (DCE) at room temperature.^{3d,6} The transient absorption spectra immediately after the electron pulse were assigned to $c\text{-1}^+ - 7^+$ and $t\text{-1}^+ - 8^+$ ⁹ formed from capture of the hole generated in the initiation step. The spectral changes and the time profiles

of S^+ are shown in Figures 1 and 2. Their characteristics are summarized in Table 1 and discussed later. The transient absorptions of $t\text{-S}^+$ decayed monotonously with first-order kinetics and did not show any shifts or spectral changes. The apparent rate constants (k_{obs}) were calculated from the decay of the transient absorptions at a wavelength λ and are shown in Figures 1 and 2.

The transient absorptions of $c\text{-1}^+$, $c\text{-2}^+$, and $c\text{-6}^+$ without a p -methoxyl group at λ decayed with k_{obs} , similarly to those of $t\text{-1}^+ - 8^+$ (Figures 1 and 2). On the other hand, formation of the band of $t\text{-3}^+ - 5^+$ and $t\text{-8}^+$ after the electron pulse was observed with decay of the band of $c\text{-3}^+ - 5^+$ and $c\text{-8}^+$ with a p -methoxyl group, respectively. For example, the transient absorption spectrum at 20 ns after the electron pulse was composed of bands of $c\text{-3}^+$ and $t\text{-3}^+$ at 530 and 500 nm, respectively (Figure 1). The band of $t\text{-3}^+$ at 500 nm increased in the range of 1 μs , while the band of $c\text{-3}^+$ at 530 nm decayed in the range of a few hundred nanoseconds and became constant in the range of 1 μs because of formation of the band of $t\text{-3}^+$. The decay profile of the band of $c\text{-3}^+$ at 530 nm was consistent with the formation profile of the band of $t\text{-3}^+$ at 500 nm. Similar time profiles were observed in the transient absorptions of $c\text{-4}^+$, $c\text{-5}^+$, and $c\text{-8}^+$. The rate constants (k_i) of the unimolecular isomerization of $c\text{-S}^+$ to $t\text{-S}^+$ were calculated from the rise in the absorption peaks of t^+ (Figures 1 and 2 and Table 2), which did not depend on the concentration of $c\text{-S}$ ($k_i = 4.5 \times 10^6$ to $1.4 \times 10^7 \text{ s}^{-1}$). The k_i value for $c\text{-8}^+$ was measured at various temperatures. From the Arrhenius plot of $\ln k_i$ and the reciprocal of temperature (T^{-1}), the activation energy and the preexponential factor were determined to be 1.3 kcal mol⁻¹ and $10^{7.5} \text{ s}^{-1}$, respectively (Figure 3).

Dimerization was observed in $1^+ - 3^+$ and $t\text{-6}^+$, because the decay of the absorption of $1^+ - 3^+$ and $t\text{-6}^+$ increased with increasing concentration of $1^+ - 3^+$ and $t\text{-6}^+$, respectively. The transient absorption of $c\text{-1}^+$ shifted to that of $t\text{-1}^+$ during the decay because of the bimolecular isomerization of $c\text{-1}^+$ to $t\text{-1}^+$ via $\sigma\text{-St}_2^+$, as reported previously.^{1c,d} Similarly, $c\text{-2}^+$ shifted to that of $t\text{-2}^+$ through bimolecular isomerization. The rate constant of the dimerization ($k_d = (2.0 - 4.3) \times 10^8 \text{ M}^{-1} \text{ s}^{-1}$) was calculated from the dependence of decay of the transient absorption of $1^+ - 3^+$ and $t\text{-6}^+$ on the concentration of $1 - 3$

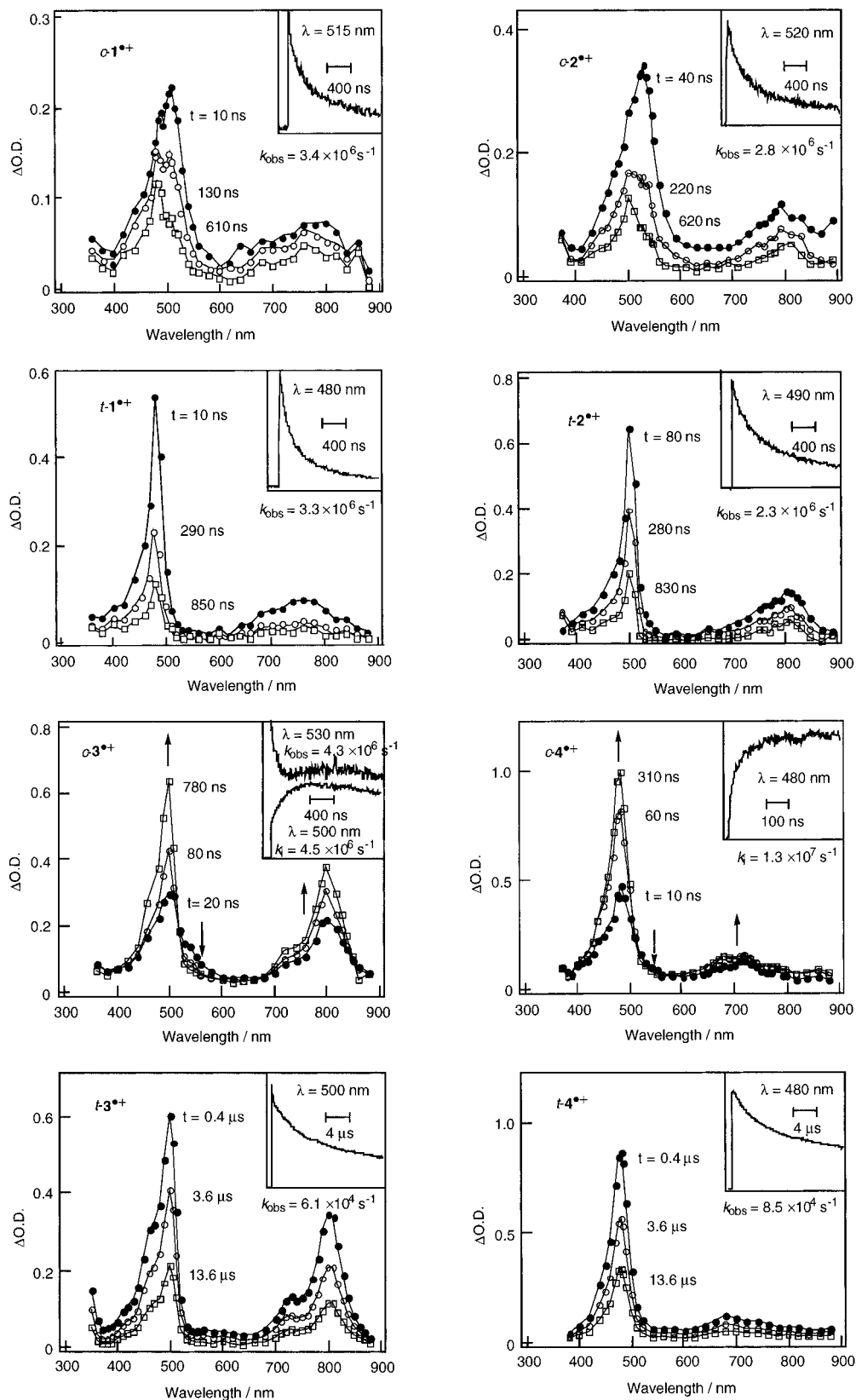


Figure 1. Transient absorption spectra of $c\text{-S}^{*\cdot+}$ and $t\text{-S}^{*\cdot+}$ ($\text{S}^{*\cdot+} = 1^{*\cdot+}\text{-}4^{*\cdot+}$) recorded at time t after an electron pulse during the pulse radiolysis of an Ar-saturated DCE solution of $c\text{-S}$ and $t\text{-S}$ ($\text{S} = 1\text{-}4$) with a concentration of 5.0×10^{-3} M at room temperature. Insets: kinetic traces illustrating the time profiles of the D_2 absorption band at a wavelength λ as a function of t . Both t and the observed rate constants (k_{obs} and k_i) are mentioned in the figure.

and $t\text{-6}$, respectively (Table 2).¹⁰ For example, plots of k_{obs} for $c\text{-1}^{*\cdot+}$, $c\text{-2}^{*\cdot+}$, or $c\text{-3}^{*\cdot+}$ vs the concentration of $c\text{-1}$, $c\text{-2}$, or $c\text{-3}$, respectively, are shown in Figure 4. When the linear plots of k_{obs} vs concentration of $c\text{-1}$ and $c\text{-2}$ were extrapolated to 0 M, the intercepts were essentially equal to k_i . However, the plots gave significantly small values of the intercepts, which indicates

that $k_i < 10^6 \text{ s}^{-1}$. No dimerization of $c\text{-6}^{*\cdot+}$ was observed, because the decay of the absorption did not depend on the concentration of $c\text{-6}$.

The transient absorption of $c\text{-7}^{*\cdot+}$ with a p -methoxyl group and a methyl group on the olefinic carbon decayed with k_{obs} according to first-order kinetics without any shifts or influence

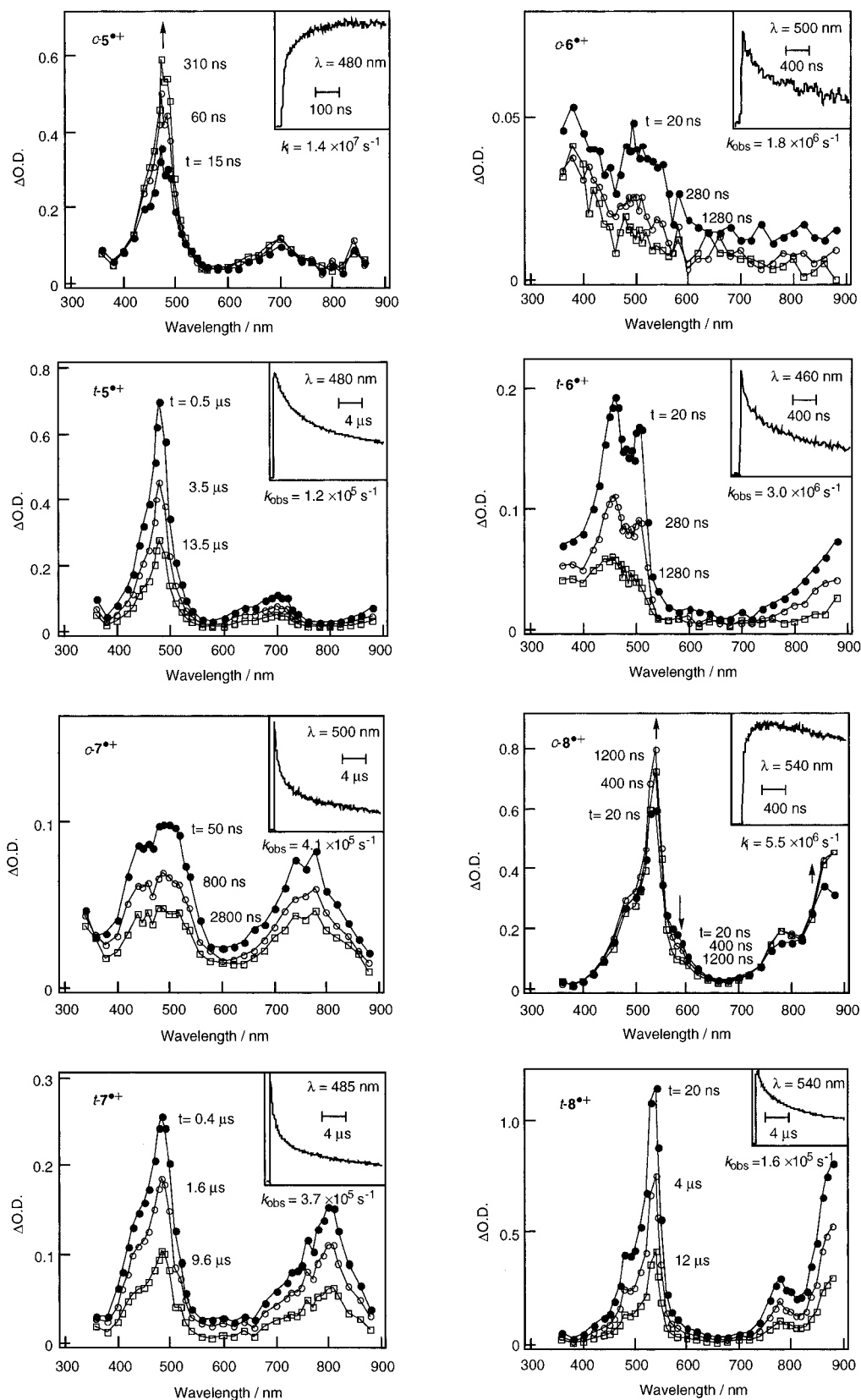


Figure 2. Transient absorption spectra of $c\text{-S}^{*+}$ and $t\text{-S}^{*+}$ ($\text{S}^{*+} = 5^{*+}\text{--}8^{*+}$) recorded at time t after an electron pulse during the pulse radiolysis of an Ar-saturated DCE solution of $c\text{-S}$ and $t\text{-S}$ ($\text{S} = 5\text{--}8$) with a concentration of 5.0×10^{-3} M at room temperature. Insets: kinetic traces illustrating the time profiles of the D_2 absorption band at a wavelength λ as a function of t . Both t and the observed rate constants (k_{obs} and k_i) are mentioned in the figure.

of the concentration. In other words, neither unimolecular isomerization nor dimerization was observed in $c\text{-7}^{*+}$ (Figure 2).

Pulse radiolyses of $t\text{-S}$ and $c\text{-S}$ were carried out in O_2 -saturated DCE at room temperature. The decay of the transient absorption of $t\text{-S}^{*+}$ was accelerated in the presence of O_2 in the

cases of $t\text{-3}^{*+}\text{--}5^{*+}$ and $t\text{-7}^{*+}$ with a p -methoxyl group. The decay rates were measured as a function of the concentration of O_2 , and the rate constant of the oxidation (k_{O_2}) was calculated to be $k_{\text{O}_2} = (1.2\text{--}4.5) \times 10^7 \text{ M}^{-1} \text{ s}^{-1}$ (Table 2). A typical example of the plot of k_{obs} vs concentration of O_2 for $t\text{-3}^{*+}$ is shown in Figure 5. On the other hand, no oxidation was

TABLE 2: Rate Constants for the Reactions of S^+ ($S^+ = 1^+ - 8^+$) in Pulse Radiolyses in DCE at Room Temperature^a

S^+	$c\text{-}S^+$			$t\text{-}S^+$	
	k_i/s^{-1}	$k_d/M^{-1} s^{-1}$	$k_{O_2}/M^{-1} s^{-1}$	$k_d/M^{-1} s^{-1}$	$k_{O_2}/M^{-1} s^{-1}$
1^+	$<10^6$	3.9×10^8	$<10^6$	3.9×10^8	$<10^6$
2^+	$<10^6$	3.4×10^8	$<10^6$	4.3×10^8	$<10^6$
3^+	4.5×10^6	2.0×10^8	nd	3.0×10^8	4.5×10^7
4^+	1.3×10^7	nd	nd	$<10^6$	4.0×10^7
5^+	1.4×10^7	nd	nd	$<10^6$	1.2×10^7
6^+	$<10^6$	$<10^6$	$<10^6$	3.4×10^8	$<10^6$
7^+	$<10^6$	$<10^6$	2.5×10^7	$<10^6$	2.8×10^7
8^+	5.5×10^6	nd	$<10^6$	$<10^6$	$<10^6$

^a k_i , calculated from the formation of $t\text{-}S^+$ at 5.0×10^{-3} M of $c\text{-}S$; k_d , measured from the dependence of the decay of S^+ on the concentration of S ; k_{O_2} , obtained from the dependence of the decay of $c\text{-}S^+$ or $t\text{-}S^+$ on the concentration of O_2 . $k_i < 10^6 s^{-1}$ denotes that the formation of $t\text{-}S^+$ was not observed. $k_d < 10^6 M^{-1} s^{-1}$ and $k_{O_2} < 10^6 M^{-1} s^{-1}$ denote that there was no dependence of the decay of $c\text{-}S^+$ or $t\text{-}S^+$ on the concentration of $c\text{-}S$, $t\text{-}S$, or O_2 .

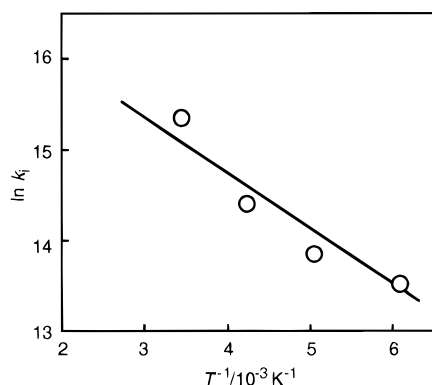


Figure 3. Arrhenius plot of $\ln k_i$ and the reciprocal of temperature (T^{-1}) for the unimolecular isomerization of $c\text{-}8^+$ to $t\text{-}8^+$ during the pulse radiolysis of an Ar-saturated DCE solution of $c\text{-}8$ (5.0×10^{-3} M).

observed on a similar time scale in $t\text{-}1^+$, $t\text{-}2^+$, and $t\text{-}6^+$ without a p -methoxyl group. For example, no effect of the concentration of O_2 on k_{obs} in $t\text{-}1^+$ is shown in Figure 5. No oxidation was also observed in $t\text{-}8^+$ with two p -methoxyl groups. Oxidation of $c\text{-}7^+$ was also observed with a k_{O_2} value similar to that for $t\text{-}7^+$, while no oxidation was observed in $c\text{-}1^+$, $c\text{-}2^+$, and $c\text{-}6^+$ without a p -methoxyl group and in $c\text{-}8^+$ with two p -methoxyl groups. In the case of $c\text{-}3^+ - 5^+$ with a p -methoxyl group, k_{O_2} could not be estimated because of the fast unimolecular isomerization of $c\text{-}3^+ - 5^+$ to $t\text{-}3^+ - 5^+$ at $k_i = 4.5 \times 10^6$ to $1.3 \times 10^7 M^{-1} s^{-1}$.

Absorption Spectra of S^+ . $c\text{-}$ and $t\text{-}2^+ - 8^+$ show two typical absorption bands in the range 400–600 and 700–1000 nm assigned to $D_2 \leftarrow D_0$ and $D_1 \leftarrow D_0$ transitions, respectively, similarly to 1^+ (Figure 1 and Table 1).⁹ Although the shape and wavelength of the absorption bands depend on the compounds, $c\text{-}S^+$ shows an absorption peak at λ_{max} at a longer wavelength than $t\text{-}S^+$, similarly to the case of $c\text{-}1^+$ and $t\text{-}1^+$. The characteristics of the absorption spectra are summarized with respect to substitution as follows.

(1) *p*-Methyl Substitution. 2^+ shows a spectrum similar to that of 1^+ , although the λ_{max} shifts at a longer wavelength of approximately 5–10 nm.

(2) *p*-Methoxyl Substitution. 3^+ , 7^+ , and 8^+ show a λ_{max} and a shoulder peak of D_1 at 700–900 nm with relatively larger molar absorption coefficients (ϵ_λ) than those of 1^+ .¹¹ $c\text{-}3^+$, $t\text{-}3^+$, and $t\text{-}8^+$ show absorption peaks of D_2 at a longer wavelength of approximately 15–60 nm than 1^+ . $t\text{-}3^+$ and $t\text{-}8^+$ show a shoulder peak of D_2 at 480 nm. $t\text{-}8^+$ also shows the two λ_{max} of D_1 at 760–900 nm. The spectrum of $c\text{-}7^+$

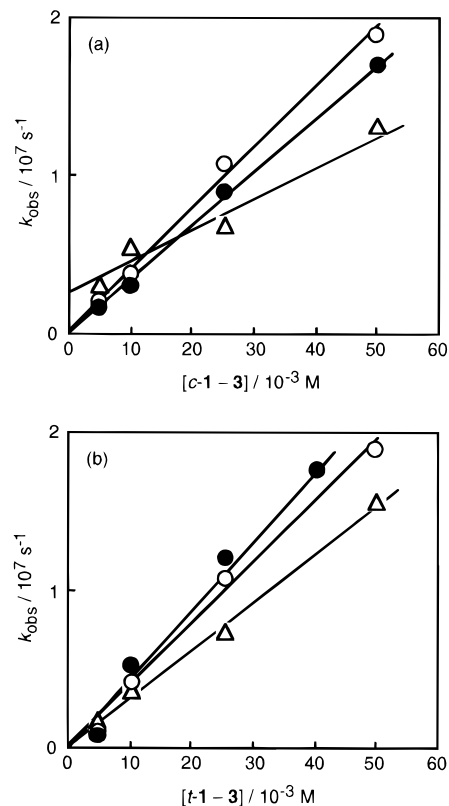


Figure 4. Plots of the observed decay rate constants (k_{obs}) of the transient absorptions of $c\text{-}1^+$ (○), $c\text{-}2^+$ (●), $c\text{-}3^+$ (□) (a) and $t\text{-}1^+$ (○), $t\text{-}2^+$ (●), $t\text{-}3^+$ (□) (b) vs concentration of $c\text{-}1$, $c\text{-}2$, $c\text{-}3$, $t\text{-}1$, $t\text{-}2$, or $t\text{-}3$ ($[c-1]$, $[c-2]$, $[c-3]$, $[t-1]$, $[t-2]$, or $[t-3]$), respectively, during the pulse radiolysis of an Ar-saturated DCE solution.

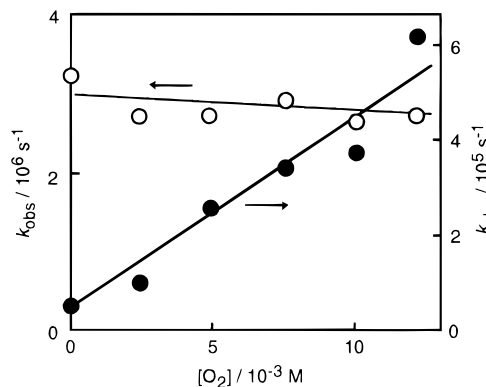


Figure 5. Plots of the observed decay rate constants (k_{obs}) of the transient absorptions of $t\text{-}1^+$ (○) or $t\text{-}3^+$ (●) vs concentration of oxygen ($[O_2]$) during the pulse radiolysis of a DCE solution of $t\text{-}1$ or $t\text{-}3$ (5.0×10^{-3} M), respectively.

was measured, while the absorption bands of $c\text{-}3^+ - 5^+$ and $c\text{-}8^+$ were not detected because $c\text{-}3^+ - 5^+$ and $c\text{-}8^+$ isomerized rapidly to $t\text{-}3^+ - 5^+$ and $t\text{-}8^+$.

The absorption spectra of $c\text{-}3^+$ and $t\text{-}3^+$ generated by γ -radiolyses of $c\text{-}3$ and $t\text{-}3$ in butyl chloride at 77 K appear similar to those observed during pulse radiolyses of $c\text{-}3^+$ and $t\text{-}3^+$ in DCE (Figure 6). Because $c\text{-}3^+$ has a larger ϵ_λ only in the range 510–670 nm than $t\text{-}3^+$, it is expected that the optical densities decrease in the range 510–670 nm but increase in other ranges because of the unimolecular isomerization of $c\text{-}3^+$ to $t\text{-}3^+$.

Measurement of the absorption spectra of $c\text{-}8^+$ and $t\text{-}8^+$ using a multichannel photodetector was also carried out in the γ -radiolyses of $c\text{-}8$ and $t\text{-}8$ in butyl chloride at 77 K. The same absorption spectrum was observed with a peak at 540 nm, which is assigned to $t\text{-}8^+$. This indicates that $c\text{-}8^+$ isomerizes to $t\text{-}8^+$

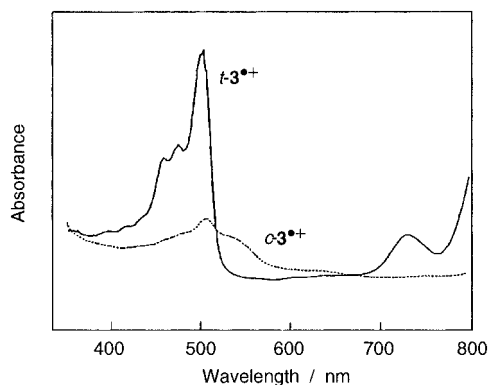


Figure 6. Absorption spectra of $c\text{-}3^{\bullet+}$ and $t\text{-}3^{\bullet+}$ measured by γ -radiolyses of butyl chloride solutions containing 5.0×10^{-3} M $c\text{-}3$ and $t\text{-}3$ at 77 K.

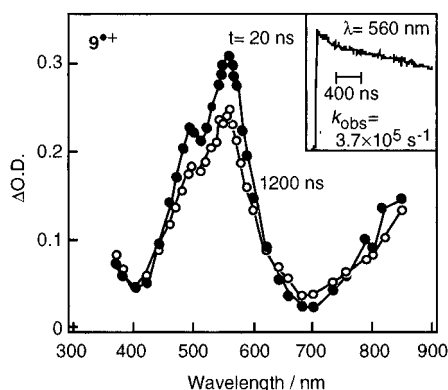


Figure 7. Transient absorption spectra of $9^{\bullet+}$ recorded at t after an electron pulse in the pulse radiolysis of an Ar-saturated DCE solution of 9 (5.0×10^{-3} M) at room temperature. Inset: kinetic trace illustrating the time profile of the D_2 absorption band at 560 nm as a function of t . Both t and the observed rate constant (k_{obs}) are mentioned in the figure.

during the spectral measurement by a multichannel photodetector even at 77 K.¹² To confirm the absorption spectrum of $c\text{-}8^{\bullet+}$, that of the 1,2-bis(4-methoxyphenyl)cyclo-1-pentene (9) radical cation was measured during the pulse radiolysis in DCE (Figure 7). 9 has a rigid planar structure, with the $c\text{-}8$ chromophore constrained structurally by the cyclopentene ring, and is stable for geometrical isomerizations as the structurally constrained derivative of $c\text{-}8$. From the $\lambda_{\text{max}} = 490$ and 560 nm and ϵ_{λ} of $9^{\bullet+}$, $c\text{-}8^{\bullet+}$ is expected to show a λ_{max} at longer wavelengths, with a smaller ϵ_{λ} than those of $t\text{-}8^{\bullet+}$ and $9^{\bullet+}$, similarly to the difference between the values for other $c\text{-}S^{\bullet+}$ and $t\text{-}S^{\bullet+}$. The absorption spectrum of $9^{\bullet+}$ collapsed on a microsecond time scale.

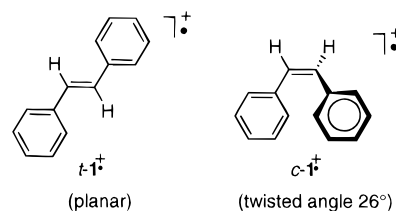
(3) *o*-Methoxyl and *m*-Methoxyl Substitution. Both $t\text{-}4^{\bullet+}$ and $t\text{-}5^{\bullet+}$ show a λ_{max} of D_2 at 480 nm, which is same as that of $t\text{-}1^{\bullet+}$, while D_1 of $t\text{-}4^{\bullet+}$ and $t\text{-}5^{\bullet+}$ is observed at 680–700 nm, with an extremely smaller ϵ_{λ} than that of $t\text{-}1^{\bullet+}$.

(4) *m,m*-Dimethoxyl Substitution. $t\text{-}6^{\bullet+}$ shows two λ_{max} of D_2 at 460 and 510 nm and a λ_{max} of D_1 at a wavelength longer than 900 nm, with a considerably small ϵ_{λ} . On the other hand, $c\text{-}6^{\bullet+}$ shows very weak and broad absorption bands in the range 360–900 nm.

(5) Methyl on the Central C=C Double Bond. $c\text{-}7^{\bullet+}$ and $t\text{-}7^{\bullet+}$ show broader absorption bands, with a smaller ϵ_{λ} than those of $t\text{-}3^{\bullet+}$.

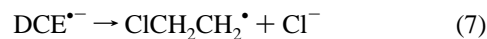
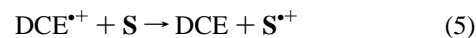
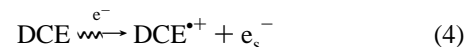
The most remarkable characteristics of the absorption spectra of $c\text{-}$ and $t\text{-}2^{\bullet+}$ – $8^{\bullet+}$ are that the λ_{max} values of $3^{\bullet+}$ – $5^{\bullet+}$ and $8^{\bullet+}$ shift to longer wavelengths with larger ϵ_{λ} values than those of $1^{\bullet+}$ (Table 1) and that $c\text{-}6^{\bullet+}$ show a λ_{max} with an extremely small ϵ_{λ} , similar to that of the 1,3-dimethoxybenzene radical cation.¹³

SCHEME 2



Discussion

Formation of $S^{\bullet+}$. It is well established that the radical cation of 1 ($1^{\bullet+}$) is formed during pulse radiolyses and γ -radiolyses in alkyl halide solutions such as DCE and butyl chloride.^{9,11,14} Absorption spectra of $c\text{-}3^{\bullet+}$ and $t\text{-}3^{\bullet+}$ generated by γ -radiolyses of $c\text{-}3$ and $t\text{-}3$ in butyl chloride at 77 K show absorption bands similar to those of $c\text{-}1^{\bullet+}$ and $t\text{-}1^{\bullet+}$: $c\text{-}3^{\bullet+}$, 420–580 with $\lambda_{\text{max}} = 500$ nm; $t\text{-}3^{\bullet+}$, 400–520 and >700 with $\lambda_{\text{max}} = 495, 730$, and >800 nm (Figure 1). Similar absorption spectra of $c\text{-}2^{\bullet+}$, $c\text{-}4^{\bullet+}$ – $8^{\bullet+}$, $t\text{-}2^{\bullet+}$, and $t\text{-}4^{\bullet+}$ – $8^{\bullet+}$ were observed in the γ -radiolyses. Therefore, $c\text{-}S^{\bullet+}$ and $t\text{-}S^{\bullet+}$ ($S^{\bullet+} = 1^{\bullet+}$ – $8^{\bullet+}$) are formed initially by hole transfer from the radical cation of DCE ($\text{DCE}^{\bullet+}$) as shown in the following initiation processes (eqs 4–7),



where e_s^- denotes a solvated electron and is stabilized by dissociative attachment to DCE.

Assignments of Absorption Bands of $S^{\bullet+}$. To study the electronic properties of $c\text{-}S^{\bullet+}$ and $t\text{-}S^{\bullet+}$, we have measured the transient absorption spectra of $c\text{-}S^{\bullet+}$ and $t\text{-}S^{\bullet+}$ during pulse radiolyses of S at room temperature (Figure 1). The spectral characteristics are shown with respect to the λ_{max} and ϵ_{λ} of D_1 and D_2 (Table 1).

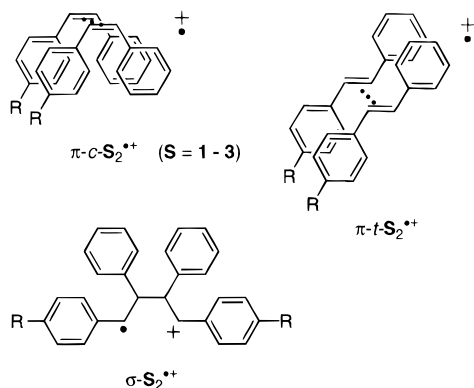
It is established that $t\text{-}1^{\bullet+}$ shows two absorption bands in the range 400–510 and 650–900 nm with a relatively sharp $\lambda_{\text{max}} = 480$ nm and a weak $\lambda_{\text{max}} = 750$ nm assigned to $D_2 \leftarrow D_0$ and $D_1 \leftarrow D_0$ transitions, respectively, while $c\text{-}1^{\bullet+}$ also shows two absorption bands in the range 400–580 and 650–900 nm with a relatively strong $\lambda_{\text{max}} = 515$ nm and a weak $\lambda_{\text{max}} = 780$ nm, respectively.⁹ The absorption bands of $c\text{-}1^{\bullet+}$ are broader and weaker than those of $t\text{-}1^{\bullet+}$, while the absorption bands of $c\text{-}1^{\bullet+}$ shift to longer wavelengths than those of $t\text{-}1^{\bullet+}$. The differences depend on the electronic configurations of D_0 , D_1 , and D_2 of $c\text{-}S^{\bullet+}$ and $t\text{-}S^{\bullet+}$. It is reported that $t\text{-}1^{\bullet+}$ has a planar structure with two benzene rings and a C=C double bond as the most stable conformation, while $c\text{-}1^{\bullet+}$ has a twist angle of 26° between the two benzene rings on the basis of MO calculations (Scheme 2).¹⁵ Therefore, delocalization of π -electrons is less in $c\text{-}1^{\bullet+}$ than in $t\text{-}1^{\bullet+}$. The energy level of D_0 is suggested to increase in $c\text{-}1^{\bullet+}$ compared that with in $t\text{-}1^{\bullet+}$.

Effects of Substituents on Electronic Properties of $2^{\bullet+}$ – $8^{\bullet+}$. On the basis of absorption spectra (Figures 1 and 2 and Table 1), the effects of substituents on the electronic properties of $2^{\bullet+}$ – $8^{\bullet+}$ are summarized as follows.

(1) *p*-Methyl ($2^{\bullet+}$) and *p*-methoxyl substitutions ($3^{\bullet+}$ – $5^{\bullet+}$, $7^{\bullet+}$, and $8^{\bullet+}$) enhance the delocalization of π -electrons of $c\text{-}1^{\bullet+}$ and $t\text{-}1^{\bullet+}$.

(2) *p*-Methoxyl substitution ($3^{\bullet+}$ – $5^{\bullet+}$ and $8^{\bullet+}$) leads to two types of $D_2 \leftarrow D_0$ and $D_1 \leftarrow D_0$ transitions. The λ_{max} values at

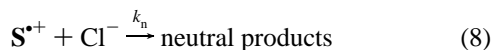
SCHEME 3



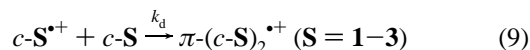
the longer wavelength of the $D_2 \leftarrow D_0$ shift to a longer wavelength in the order $t\text{-}1^{+\bullet}$, $t\text{-}2^{+\bullet}$, $t\text{-}3^{+\bullet}$, $c\text{-}1^{+\bullet}$, $c\text{-}2^{+\bullet}$, $c\text{-}3^{+\bullet}$, $t\text{-}8^{+\bullet}$, and $c\text{-}8^{+\bullet}$. This order indicates that the λ_{max} shifts to longer wavelength with increasing deviation from the planarity of the two benzene rings and the C=C double bond induced by increasing the single-bond character of the C=C double bond or the charge-spin separation character because of the *p*-methoxy group, as discussed below.

(3) *o,m*-Dimethoxy substitution ($4^{+\bullet}$, $5^{+\bullet}$), *m,m*-dimethoxy substitution ($6^{+\bullet}$), and methyl substitution on the central C=C double bond ($7^{+\bullet}$) interfere with the delocalization of π -electrons of $t\text{-}1^{+\bullet}$ because of the steric repulsion of the planar structure. The significant weak broad absorptions of $6^{+\bullet}$ suggest that $6^{+\bullet}$, particularly $c\text{-}6^{+\bullet}$, has a twisted structure with the 3,5-dimethoxyphenyl ring rotating relative to the C=C double bond.

Dimerization of $c\text{-}S^{+\bullet}$. The decay of $c\text{-}1^{+\bullet}$ has been analyzed by neutralization with Cl^- formed from dissociative electron attachment to DCE (eq 7) at a rate constant of $k_n = 1.6 \times 10^{11} \text{ M}^{-1} \text{ s}^{-1}$ (eq 8) when the concentration of $c\text{-}1$ is low (10^{-4} M).^{3d,11}



It is reported that the dimerization of $c\text{-}1^{+\bullet}$ with $c\text{-}1$ occurs at a rate constant of $k_d^c = 3.5 \times 10^8 \text{ M}^{-1} \text{ s}^{-1}$ at room temperature to form a π -type dimer radical cation of $c\text{-}1$ ($\pi\text{-}(c\text{-}1)_2^{+\bullet}$, eq 9), which changes to a σ -type dimer radical cation of 1 ($\sigma\text{-}1_2^{+\bullet}$, eq 10) (Scheme 3) on the basis of spectroscopic measurements



during the pulse radiolyses and γ -radiolyses of $c\text{-}1$ and 1,2,3,4-tetraphenylcyclobutanes as precursors of the σ -dimer model compounds in DCE at room temperature and in butyl chloride at 77 K.^{3d} The unimolecular isomerization of $c\text{-}1^{+\bullet}$ to $t\text{-}1^{+\bullet}$ does not occur, although the bimolecular isomerization of $c\text{-}1^{+\bullet}$ to $t\text{-}1^{+\bullet}$ is proposed to occur through $\sigma\text{-}1_2^{+\bullet}$ on the time scale of 100–300 ns with the concentration of $(5\text{--}10) \times 10^{-3} \text{ M}$ at room temperature.^{3c,d} Thermally unstable $\sigma\text{-}1_2^{+\bullet}$ decomposes rapidly into the thermodynamically stabler $t\text{-}1^{+\bullet}$ and $t\text{-}1$ (eq 11), as proposed.^{3c,d} Therefore, the bimolecular isomerization is enhanced with increasing concentration of $c\text{-}1$.

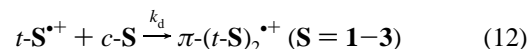


Similarly, concentration effects suggest that the bimolecular isomerizations of $c\text{-}2^{+\bullet}$ and $c\text{-}3^{+\bullet}$ to $t\text{-}2^{+\bullet}$ and $t\text{-}3^{+\bullet}$ involve the dimerization of $c\text{-}2^{+\bullet}$ and $c\text{-}3^{+\bullet}$ to form $\pi\text{-}(c\text{-}2)_2^{+\bullet}$ and $\pi\text{-}(c\text{-}3)_2^{+\bullet}$ and then $\sigma\text{-}2_2^{+\bullet}$ and $\sigma\text{-}3_2^{+\bullet}$ (eqs 9 and 10, respectively),

although no direct evidence for them was observed. Similar values of k_d^c for $c\text{-}1^{+\bullet}$ – $c\text{-}3^{+\bullet}$ suggest that *p*-methyl and *p*-methoxy substitutions have little effect on the dimerization of $c\text{-}S^{+\bullet}$. Structures of $\pi\text{-}(c\text{-}2)_2^{+\bullet}$ and $\pi\text{-}(c\text{-}3)_2^{+\bullet}$ are assumed to overlap between the same benzene rings for a greater perturbation of the π -orbitals, as shown in Scheme 3. It is suggested that $\sigma\text{-}2_2^{+\bullet}$ decomposes rapidly into the thermodynamically stabler $t\text{-}2^{+\bullet}$ and $t\text{-}2$, while $\sigma\text{-}3_2^{+\bullet}$ decomposes slowly into $t\text{-}3^{+\bullet}$ and $t\text{-}3$ (eq 11) because there is no effect of the concentration of $c\text{-}3$ on the formation of the absorption of $t\text{-}3^{+\bullet}$. This is probably attributed to *p*-methoxy substitution, which makes $\sigma\text{-}3_2^{+\bullet}$ stable toward β -fission because of electron donating to the positive charge and radical centers.

The decay of the absorption of other $c\text{-}S^{+\bullet}$ at higher concentrations could not be performed, because the decay was too fast to be detected within the experimental limits, or the concentration of $c\text{-}4\text{--}8$ could not be increased because of low solubilities in DCE. The k_d^c value for $c\text{-}8^{+\bullet}$ with a *p*-methoxy group is expected to be $10^8 \text{ M}^{-1} \text{ s}^{-1}$ from analogy with $c\text{-}3^{+\bullet}$, while the steric hindrance due to the twisted structure with the 3,5-dimethoxyphenyl ring rotating relative to the C=C double bond and to the methyl group on the olefinic carbon probably inhibits the dimerization of $c\text{-}6^{+\bullet}$ and $7^{+\bullet}$, respectively.

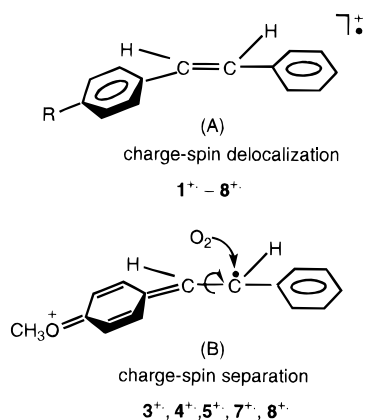
Dimerization of $t\text{-}S^{+\bullet}$. Similarly to $c\text{-}1^{+\bullet}$, $t\text{-}1^{+\bullet}$ decays via neutralization with Cl^- (eq 8) and dimerization with $t\text{-}1$ at a rate constant of $k_d^t = 3.9 \times 10^8 \text{ M}^{-1} \text{ s}^{-1}$ to form a π -type dimer radical cation of $t\text{-}1$ ($\pi\text{-}(t\text{-}1)_2^{+\bullet}$, eq 12) with overlapping of π -electrons between the two benzene rings of $t\text{-}1^{+\bullet}$ and $t\text{-}1$ (Scheme 3).^{3d,11} Neither the unimolecular nor the bimolecular isomerization of $t\text{-}1^{+\bullet}$ to $c\text{-}1^{+\bullet}$ occurs. It is found that $\pi\text{-}(t\text{-}1)_2^{+\bullet}$ generated at 77 K converts to $\sigma\text{-}1_2^{+\bullet}$ upon warming (eq 13) and finally decomposes into the thermodynamically stabler $t\text{-}1^{+\bullet}$ and $t\text{-}1$ (eq 11) on the basis of spectroscopic measurements as discussed above for $c\text{-}1^{+\bullet}$.^{3d}



$t\text{-}2^{+\bullet}$, $t\text{-}3^{+\bullet}$, and $t\text{-}6^{+\bullet}$ show behavior similar to that of $t\text{-}1^{+\bullet}$ (Table 2). Similar k_d^t values for $t\text{-}1^{+\bullet}$ – $t\text{-}3^{+\bullet}$ and $t\text{-}6^{+\bullet}$ suggest that *p*-methyl and *m*-methoxy substitutions have little effect on the dimerization of $t\text{-}S^{+\bullet}$ and that a similar dimerization mechanism has been suggested (eqs 11–13).¹⁶ On the other hand, the decay rates of the absorption bands of $t\text{-}4^{+\bullet}$, $t\text{-}5^{+\bullet}$, $t\text{-}7^{+\bullet}$, and $t\text{-}8^{+\bullet}$ were much slower than those of $t\text{-}1^{+\bullet}$ – $3^{+\bullet}$ and $t\text{-}6^{+\bullet}$, because the decay rate did not change with varying concentration (5×10^{-3} – 10^{-1} M) of $t\text{-}4$, $t\text{-}5$, $t\text{-}7$, and $t\text{-}8$, respectively. Therefore, dimerizations of $t\text{-}4^{+\bullet}$, $t\text{-}5^{+\bullet}$, $t\text{-}7^{+\bullet}$, and $t\text{-}8^{+\bullet}$ do not occur. The dimerization occurs even in $t\text{-}3^{+\bullet}$ with a large k_d^t value but not in $t\text{-}4^{+\bullet}$, $t\text{-}5^{+\bullet}$, and $t\text{-}7^{+\bullet}$; therefore, it is suggested that the dimerization involves the initial formation of a π -complex with overlapping of the two benzene rings and that the π -complex formation is inhibited by steric hindrance of the substituents on the benzene rings and olefinic carbons.

Enhancements of Unimolecular Isomerization and Oxidation by Charge–Spin Separation (Effect of *p*-Methoxy Substituent). In contrast to $c\text{-}1^{+\bullet}$ and $2^{+\bullet}$, the unimolecular isomerization of $c\text{-}3^{+\bullet}$ – $5^{+\bullet}$ and $c\text{-}8^{+\bullet}$ having a *p*-methoxy group occurs to yield $t\text{-}3^{+\bullet}$ – $5^{+\bullet}$ and $t\text{-}8^{+\bullet}$, respectively. The k_i value for $c\text{-}3^{+\bullet}$ is almost equivalent to that for $c\text{-}8^{+\bullet}$, while those for $c\text{-}4^{+\bullet}$ and $c\text{-}5^{+\bullet}$ are larger than those for $c\text{-}3^{+\bullet}$ and $c\text{-}8^{+\bullet}$. Neither the unimolecular nor the bimolecular isomerization occurs in $c\text{-}6^{+\bullet}$ and $c\text{-}7^{+\bullet}$. The oxidation of $t\text{-}3^{+\bullet}$ – $5^{+\bullet}$ and $7^{+\bullet}$ having a *p*-methoxy group with O_2 occurs at $k_{\text{O}_2} = (1.2\text{--}4.5) \times 10^7 \text{ M}^{-1} \text{ s}^{-1}$, while the oxidation does not occur in $c\text{-}1^{+\bullet}$, $c\text{-}2^{+\bullet}$, or

SCHEME 4



$c\text{-}6^+$ without a *p*-methoxyl group and in $t\text{-}8^+$ with two *p*-methoxyl groups. The unimolecular isomerization and the oxidation with O_2 are remarkably enhanced in $3^+ - 5^+$ and 7^+ with a *p*-methoxyl group.

On the basis of these experimental results, it is clearly shown that a *p*-methoxyl group as an electron-donating substituent on the benzene ring remarkably changes the reactivities of $1^+ - 8^+$. It is reported that $t\text{-}1^+$ has a planar structure with the two benzene rings and the $\text{C}=\text{C}$ double bond as the most stable conformation, while $c\text{-}1^+$ has a twist angle of 26° between the two benzene rings on the basis of MO calculations.¹⁵ Although the positive charge and unpaired electron are delocalized on the singly occupied molecular orbital (SOMO) involving π -orbitals of sp^2 carbon atoms and the *n*-orbital of the oxygen atom of the *p*-methoxyl group in $1^+ - 8^+$, as shown in structure A, a quinoid-type structure, B, is considered to contribute in $3^+ - 5^+$, 7^+ , and 8^+ with a *p*-methoxyl group but not in 1^+ , 2^+ , and 6^+ without a *p*-methoxyl group (Scheme 4).¹⁷ Alternatively, the *n*-orbital of the oxygen atom of the *p*-methoxyl group and the π -orbital of the olefinic β -carbon participate considerably in the SOMO of $3^+ - 5^+$, 7^+ , and 8^+ . Therefore, it is suggested that *p*-methoxyl substitution in $3^+ - 5^+$, 7^+ , and 8^+ causes separation and localization of the positive charge on the oxygen atom of the *p*-methoxyl group and an unpaired electron on the olefinic β -carbon (charge-spin separation), which induces a twisted conformation with a large twist angle and $\text{C}-\text{C}$ single-bond character for the central $\text{C}=\text{C}$ double bond in B. On the other hand, such charge-spin separation is less important in 1^+ , 2^+ , and 6^+ than in $3^+ - 5^+$, 7^+ , and 8^+ .

The occurrence of unimolecular isomerization and oxidation in $3^+ - 5^+$, 7^+ , and 8^+ , the large G values of the formation of $t\text{-}3 - 5$ in the γ -radiolyses of $c\text{-}3 - 5$ in Ar-saturated DCE,¹⁸ and the regioselective formation of 4-methoxybenzyl phenyl ketone in the γ -radiolysis of $t\text{-}3$ in O_2 -saturated DCE¹⁸ are consistent with the order of k_i and k_{O_2} and charge-spin separation induced by the *p*-methoxyl group in $3^+ - 5^+$, 7^+ , and 8^+ . It is suggested that distonic radical cations known in the gas phase¹⁹ can be used to explain the reactivities of radical cations even in solution.²⁰

Neither the unimolecular isomerization of $c\text{-}7^+$ nor the oxidation of $t\text{-}8^+$ occurred, although 7^+ and 8^+ have a *p*-methoxyl group. These are possibly explained in terms of a barrier to the twisting of the $\text{C}=\text{C}$ double bond and the spin density on the olefinic carbon, respectively. The contribution of B is decreased by the electron-donating methyl group on the olefinic carbon; therefore, it is suggested that the single-bond character of the $\text{C}=\text{C}$ double bond is lower in $c\text{-}7^+$ than in $c\text{-}3^+$ and that the barrier to the twisting of the $\text{C}=\text{C}$ double bond is higher in $c\text{-}7^+$ than in $c\text{-}3^+$. An unpaired electron

TABLE 3: Oxidation Potentials ($E_{1/2}^{\text{ox}}$) of $c\text{-S}$ and $t\text{-S}$ ($S = 1-6$) and Difference between $E_{1/2}^{\text{ox}}(c\text{-S})$ and $E_{1/2}^{\text{ox}}(t\text{-S})^a$

S	R of $\text{RCH}=\text{CHPh}$	$E_{1/2}^{\text{ox}}(c\text{-S})/\text{V}$	$E_{1/2}^{\text{ox}}(t\text{-S})/\text{V}$	$\Delta E_{1/2}^{\text{ox}}(c-t)/\text{V}$
1	Ph	1.25	1.14	0.11
2	4- $\text{CH}_3\text{C}_6\text{H}_4$	1.16	1.05	0.11
3	4- $\text{CH}_3\text{OC}_6\text{H}_4$	0.94	0.82	0.12
4	2,4- $(\text{CH}_3\text{O})_2\text{C}_6\text{H}_3$	0.80	0.64	0.16
5	3,4- $(\text{CH}_3\text{O})_2\text{C}_6\text{H}_3$	0.87	0.72	0.15
6	3,5- $(\text{CH}_3\text{O})_2\text{C}_6\text{H}_3$	1.23	1.03	0.20

^a Half-wave oxidation potentials ($E_{1/2}^{\text{ox}}(c\text{-S})$ and $E_{1/2}^{\text{ox}}(t\text{-S})$) of $c\text{-S}$ and $t\text{-S}$ at 1.0×10^{-2} M, reference electrode of Ag/AgNO_3 , supporting electrolyte of 10^{-1} M tetraethylammonium tetrafluoroborate in acetonitrile; $\Delta E_{1/2}^{\text{ox}}(c-t) = E_{1/2}^{\text{ox}}(c\text{-S}) - E_{1/2}^{\text{ox}}(t\text{-S})$.

appears on the olefinic carbon on the side of the *p*-methoxyphenyl group in 3^+ because of contribution of B, while it appears on both olefinic carbons in 8^+ with two symmetrical *p*-methoxyl groups. Therefore, the density of an unpaired electron on the olefinic carbon in $t\text{-}8^+$ is lower than that in $t\text{-}3^+$.

Neither the unimolecular $c-t$ isomerization nor the oxidation of $c\text{-}6^+$ occurred. It should be noted that $c\text{-}6^+$ shows a λ_{max} with an extremely small ϵ_λ compared with $c\text{-}1^+ - 5^+$, $c\text{-}7^+$, and $c\text{-}8^+$, but similar to the ϵ_λ value of the 1,3-dimethoxybenzene radical cation.¹³ These results may be interpreted by a twisted structure with the 3,5-dimethoxyphenyl ring rotating relative to the $\text{C}=\text{C}$ double bond, because a quinoid-type structure, B, is not possible in $c\text{-}6^+$ having an *m*-methoxyl group.

Tokumaru and his co-workers reported that $k_i = 3 \times 10^5 \text{ s}^{-1}$ for radical cations of *cis*-4,4'-dibromostilbene ($c\text{-}10^+$) and *cis*-4,4'-dimethylstilbene ($c\text{-}11^+$) and $k_i > 3 \times 10^5 \text{ s}^{-1}$ for $c\text{-}8^+$.^{2c} They proposed that the unimolecular $c-t$ isomerization might be accelerated by reduction of the electron density on the unsaturated linkage induced by the substituents on the basis of lower coupling constants of the $\alpha\text{-H}$ of $t\text{-}10$ and $t\text{-}11$ having *p*-substituents rather than that of $t\text{-}1$ itself in ESR studies.²¹ They also proposed that the oxidation depends on the structures of the olefins, because the k_{O_2} values varied over a wide range.^{4e,f} The k_i values for $c\text{-}3^+ - 5^+$ and $c\text{-}8^+$ are 1 or 2 orders larger than those for $c\text{-}10^+$ and $c\text{-}11^+$,^{2c} as shown in Table 2. Remarkable enhancements of the unimolecular $c-t$ isomerization by *p*-methoxyl substitution are explained by charge-spin separation in $c\text{-}3^+ - 5^+$ and $c\text{-}8^+$.

The k_i value for $c\text{-}8^+$ was measured at various temperatures. From the Arrhenius plot of $\ln k_i$ and the reciprocal of the temperature (T^{-1}) the activation energy (E_a) and the preexponential factor (A) were determined to be $1.3 \text{ kcal mol}^{-1}$ and $10^{7.5} \text{ s}^{-1}$, respectively, which are smaller than $E_a = 7.7 \text{ kcal mol}^{-1}$ and $A = 10^{11 \pm 2} \text{ s}^{-1}$ for $c\text{-}10^+$ and $E_a = 3.3 \text{ kcal mol}^{-1}$ and $A = 10^{9 \pm 2} \text{ s}^{-1}$ for $c\text{-}11^+$.^{2c} This result is consistent with the larger value of k_i for $c\text{-}8^+$ than for $c\text{-}10^+$ and $c\text{-}11^+$ and suggests that E_a predominantly controls the unimolecular isomerization. On the basis of the differences in oxidation potentials between $c\text{-S}$ and $t\text{-S}$ (Table 3) and E_a values, the energy barrier is too high to be overcome in the isomerization of $t\text{-S}^+$ to $c\text{-S}^+$ ($11-14 \text{ kcal mol}^{-1}$). This makes the isomerization one-way from $c\text{-S}^+$ to $t\text{-S}^+$ in 1-6.

The rate constant of free radical- O_2 reactions has been reported for several free radicals and found to be nearly equal to the diffusion rate constant (k_{diff}). For example, $k_{\text{O}_2} = 2.4 \times 10^9 \text{ M}^{-1} \text{ s}^{-1}$ for the benzyl radical- O_2 reaction is similar to $k_{\text{diff}} = 6.7 \times 10^9 \text{ M}^{-1} \text{ s}^{-1}$ in cyclohexane.²² On the other hand, values of $k_{\text{O}_2} = (1.2-4.5) \times 10^7 \text{ M}^{-1} \text{ s}^{-1}$ for the oxidation of $t\text{-}3^+ - 5^+$ and $t\text{-}7^+$ are found to be 2 orders smaller than k_{O_2} for free radicals and $k_{\text{diff}} = 7.8 \times 10^9 \text{ M}^{-1} \text{ s}^{-1}$ in DCE. This suggests that an unpaired electron is not completely localized

on the olefinic carbon in $t\text{-}3^{+\bullet}-5^{+\bullet}$ and $t\text{-}7^{+\bullet}$ and that the positive charge interferes with the reactivity of $t\text{-}3^{+\bullet}-5^{+\bullet}$ and $t\text{-}7^{+\bullet}$ as a radical toward O_2 because of the electrophilic character of O_2 .

Conclusions

It is concluded that $c\text{-}3^{+\bullet}-5^{+\bullet}$ and $c\text{-}8^{+\bullet}$ with a *p*-methoxyl group generated by pulse radiolyses or γ -radiolyses isomerize unimolecularly to the corresponding $t\text{-}S^{+\bullet}$ at a unimolecular rate constant of $k_1 = 4.5 \times 10^6$ to $1.4 \times 10^7 \text{ s}^{-1}$, while $t\text{-}3^{+\bullet}-5^{+\bullet}$ and $7^{+\bullet}$ with a *p*-methoxyl group are oxidized with O_2 at a bimolecular rate constant of $k_{\text{O}_2} = (1.2\text{--}4.5) \times 10^7 \text{ M}^{-1} \text{ s}^{-1}$. On the other hand, neither the unimolecular isomerization from $t\text{-}S^{+\bullet}$ to $c\text{-}S^{+\bullet}$ nor the oxidation with O_2 occurs in $t\text{-}S^{+\bullet}$ without a *p*-methoxyl group.

It should be noted that an unpaired electron is not completely localized on the olefinic carbon in $t\text{-}3^{+\bullet}-5^{+\bullet}$ and $7^{+\bullet}$ and that a positive charge interferes with the reactivity of $t\text{-}3^{+\bullet}-5^{+\bullet}$ and $7^{+\bullet}$ as a radical toward O_2 because of the electrophilic character of O_2 . The present work is the first example to clarify that the reactivities of stilbene radical cations are controlled predominantly by charge-spin separation induced by *p*-methoxyl substitution.

Acknowledgment. We wish to thank the members of the Radiation Laboratory of ISIR, Osaka University, for running the linear accelerator. This work was partly supported by a Grant-in-Aid (No. 07455341) from the Ministry of Education, Science, Sport and Culture of Japan.

References and Notes

- Reviews: (a) Fox, M. A., Chanon, M., Eds. *Photoinduced Electron Transfer*; Elsevier: Amsterdam, The Netherlands, 1988. (b) Mattes, S. L.; Farid, S. In *Organic Photochemistry*; Padwa, A., Ed.; Marcel Dekker: New York, 1983; Vol. 6, pp 233–326. (c) Chanon, M.; Ebersson, L. In *Photoinduced Electron Transfer*; Fox, M. A., Chanon, M., Eds.; Elsevier: Amsterdam, The Netherlands, 1988; Part C, Chapter 4. (d) Lewis, F. D. In *Photoinduced Electron Transfer*; Fox, M. A., Chanon, M., Eds.; Elsevier: Amsterdam, The Netherlands, 1988; Part C, Chapter 4. (e) Yoon, U. C.; Mariano, P. S. *Acc. Chem. Res.* **1992**, *25*, 233. (f) Parker, V. D. *Acc. Chem. Res.* **1984**, *17*, 243. (g) Ebersson, L. *Adv. Phys. Org. Chem.* **1982**, *18*, 79. (h) Mizuno, K.; Otsuji, Y. In *Topics in Current Chemistry*; Springer: Berlin, 1994; Vol. 169, pp 301–346. (i) Lopez, L. In *Topics in Current Chemistry*; Mattay, J., Ed.; Springer: Berlin, 1990; Vol. 156, p 1. (k) Mattay, J. In *Topics in Current Chemistry*; Mattay, J., Ed.; Springer: Berlin, 1990; Vol. 156, p 219. (l) Mariano, P. S.; Stavinocha, J. L. In *Synthetic Organic Chemistry*; Horspool, W. M., Ed.; New York, 1984; p 145. (m) Mattay, J. *Angew. Chem., Int. Ed. Engl.* **1987**, *26*, 825. (n) Kavarnos, G. J.; Turro, N. J. *Chem. Rev.* **1986**, *86*, 401. (o) Mattay, J. *Synthesis* **1989**, 233. (p) Ledwith, A. *Acc. Chem. Res.* **1972**, *5*, 133. (q) Pac, C. *Pure Appl. Chem.* **1986**, *58*, 1249.
- (a) Lewis, F. D.; Dykstra, R. E.; Gould, I. R.; Farid, S. *J. Phys. Chem.* **1988**, *92*, 7042. (b) Lewis, F. D.; Bedell, A. M.; Dykstra, R. E.; Elbert, J. E.; Gould, I. R.; Farid, S. *J. Am. Chem. Soc.* **1990**, *112*, 8055. (c) Kuriyama, Y.; Arai, T.; Sakuragi, H.; Tokumaru, K. *Chem. Phys. Lett.* **1990**, *173*, 253.
- (a) Lewis, F. D.; Petisce, J. R.; Oxman, J. D.; Nepras, M. J. *J. Am. Chem. Soc.* **1985**, *107*, 203. (b) Akaba, R.; Sakuragi, H.; Tokumaru, K. *Chem. Phys. Lett.* **1990**, *174*, 80. (c) Kuriyama, Y.; Sakuragi, H.; Tokumaru, K.; Yoshida, Y.; Tagawa, S. *Bull. Chem. Soc. Jpn.* **1993**, *66*, 1852. (d) Tojo, S.; Morishima, K.; Ishida, A.; Majima, T.; Takamuku, S. *Bull. Chem. Soc. Jpn.* **1995**, *68*, 958.
- (a) Ericksen, J.; Foote, C. S. *J. Am. Chem. Soc.* **1980**, *102*, 6083. (b) Manring, L. E.; Ericksen, J.; Foote, C. S. *J. Am. Chem. Soc.* **1980**, *102*, 4275. (c) Spada, L. T.; Foote, C. S. *J. Am. Chem. Soc.* **1980**, *102*, 391. (d) Lewis, F. D.; Petisce, J. R.; Oxman, J. D.; Nepras, M. J. *J. Am. Chem. Soc.* **1985**, *107*, 203. (e) Yamashita, T.; Tsurusako, T.; Nakamura, N.; Yasuda, M.; Shima, K. *Bull. Chem. Soc. Jpn.* **1993**, *66*, 857. (f) Tsuchiya, M.; Ebbesen, T. W.; Nishimura, Y.; Sakuragi, H.; Tokumaru, K. *Chem. Lett.* **1987**, 2121. (g) Konuma, S.; Aihara, S.; Kuriyama, Y.; Misawa, H.; Akaba, R.; Sakuragi, H.; Tokumaru, K. *Chem. Lett.* **1991**, 1897. (h) Inoue, T.;

Koyama, K.; Matsuoka, T.; Tsutsumi, S. *Bull. Chem. Soc. Jpn.* **1967**, *40*, 162. (i) Futamura, S.; Ohta, H.; Kamiya, Y. *Chem. Lett.* **1982**, 381.

(5) Tokumaru and his co-workers reported that $t\text{-}1^{+\bullet}$ reacts toward O_2 at a rate constant of $k_{\text{O}_2} = 1.3 \times 10^6 \text{ M}^{-1} \text{ s}^{-1}$ on the basis of the dependence of the decay of the absorption of $t\text{-}1^{+\bullet}$ on the initial concentration of $t\text{-}1^{+\bullet}$, which changed with varying laser intensity in the laser flash photolysis of 9-cyanoanthracene-*t*-1 in DMSO.^{4f,g} They proposed that the oxidation depends on the structures of the olefins, because the k_{O_2} values varied over a wide range, $k_{\text{O}_2} = 1.3 \times 10^6$, 7.2×10^5 , and $2.6 \times 10^8 \text{ M}^{-1} \text{ s}^{-1}$ for $t\text{-}1^{+\bullet}$, $t\text{-}8^{+\bullet}$, and the radical cation of (*E*)-2,3-diphenyl-2-butene, respectively.

(6) Tojo, S.; Morishima, K.; Ishida, A.; Majima, T.; Takamuku, S. *J. Org. Chem.* **1995**, *60*, 4684.

(7) Maccarone, E.; Mammo, A.; Perrini, G.; Torre, M. *J. Chem. Soc., Perkin Trans. 2* **1981**, 324.

(8) Mueller, G. P.; Fleckenstein, J. G.; Tallent, W. H. *J. Am. Chem. Soc.* **1951**, *73*, 2651.

(9) Hamill, W. *Radical Ions*; Kaiser, E. T., Kevan, L., Eds.; New York Interscences: New York, 1968; p 405. Shida, T.; Hamill, W. *J. Chem. Phys.* **1966**, *44*, 2375. Shida, T. *Electronic Absorption Spectra of Radical Ions*; Elsevier: Amsterdam, The Netherlands, 1988; p 113.

(10) (a) It might be suggested that the rate constant from the slopes of the plots in Figure 4 should be analyzed not only with dimerization but also with regeneration of $S^{+\bullet}$ from the dimer radical cations formed by the dimerization. However, the contribution of the formation of $S^{+\bullet}$ from the dimer radical cations is negligibly small at the initial period of the decay of the transient absorption of $S^{+\bullet}$ ($1^{+\bullet}-3^{+\bullet}$ and $t\text{-}6^{+\bullet}$), where the concentration of the dimer radical cations is much lower than that of $S^{+\bullet}$. Therefore, the decay can be analyzed with the dimerization at the initial period. Because k_{obs} values were obtained in the initial period, the plots of k_{obs} vs concentration of **S** gave linear lines from which the rate constants of dimerization were calculated (Figure 4). (b) The dimerization was also observed in $t\text{-}8^{+\bullet}$ on the basis of electrochemical measurements, although the rate constant of $k_{\text{d}} = (3.4\text{--}5) \times 10^3 \text{ M}^{-1} \text{ s}^{-1}$ was too small to be observed under the present conditions in this study. Steckhan, E. *J. Am. Chem. Soc.* **1978**, *100*, 3526. Burgbacher, G.; Schaefer, H. *J. Am. Chem. Soc.* **1979**, *101*, 7590.

(11) Yamamoto, Y.; Aoyama, T.; Hayashi, K. *J. Chem. Soc., Faraday Trans. 1* **1988**, *84*, 2209.

(12) Such *c*-*t* isomerization has also been observed in $c\text{-}1^{+\bullet}$ during the absorption measurement by a multichannel photodetector at 77 K. It is considered that photochemical isomerization of $c\text{-}1^{+\bullet}$ to $t\text{-}1^{+\bullet}$ occurs quantitatively upon irradiation of monitor light from the multichannel photodetector. Similar to $c\text{-}1^{+\bullet}$, $c\text{-}8^{+\bullet}$ could not be detected even at 77 K by a multichannel photodetector.^{3d}

(13) Takamuku, S.; Komitsu, S.; Toki, S. *Radiat. Phys. Chem.* **1989**, *34*, 553.

(14) Arai, S.; Grev, D. A.; Dorfman, L. M. *J. Chem. Phys.* **1967**, *46*, 2572.

(15) Kikuchi, O.; Oshiyama, T.; Takahashi, O.; Tokumaru, K. *Bull. Chem. Soc. Jpn.* **1992**, *65*, 2267.

(16) The dimerization of $3^{+\bullet}$ has been reported to yield a dimer in the anodic oxidation of **3** in the presence of acetic acid and sodium acetate in acetonitrile. Ebersson, L.; Parker, V. D. *Acta Chem. Scand.* **1970**, *24*, 3553.

(17) It might be suggested that Scheme 4 should be replaced by a series of canonical valence bond representations including a quinoid-type structure, B, which is favorable because of the stabilization of the positive charge by the *p*-methoxyl group. Because the contribution of B can critically explain both the unimolecular isomerization and the oxidation in $3^{+\bullet}-5^{+\bullet}$, $7^{+\bullet}$, and $8^{+\bullet}$ with a *p*-methoxyl group, B with charge-spin separation is shown in Scheme 4.

(18) Product analyses were performed in γ -radiolyses of **S** (**S** = **1**–**8**) by a ^{60}Co γ source in Ar- or O_2 -saturated DCE ($1.0 \times 10^{-2} \text{ M}$) at room temperature. $t\text{-}3\text{--}5$ were formed in high yields in γ -radiolyses of $c\text{-}3\text{--}5$ in Ar-saturated DCE, and 4-methoxybenzyl phenyl ketone was regioselectively formed in γ -radiolysis of **3** in O_2 -saturated DCE, although the details will be published elsewhere.

(19) (a) Yates, B. F.; Bouma, W. J.; Radom, L. *J. Am. Chem. Soc.* **1984**, *106*, 5805. (b) Yates, B. F.; Bouma, W. J.; Radom, L. *Tetrahedron* **1986**, *22*, 6225. (c) Hammerum, S. *Mass Spectrom. Rev.* **1988**, *7*, 123. Stirk, K. M.; Kiminkinen, L. K. M.; Kenttämää, H. I. *Chem. Rev.* **1992**, *92*, 1649. (d) Smith, R. L.; Chyall, L. J.; Chou, P. K.; Kenttämää, H. I. *J. Am. Chem. Soc.* **1994**, *116*, 781.

(20) (a) Tojo, S.; Toki, S.; Takamuku, S. *J. Org. Chem.* **1991**, *56*, 6240. (b) Brede, O.; David, F.; Steenken, S. *J. Chem. Soc., Perkin Trans. 2* **1995**, 23.

(21) Bonazzola, L.; Michaut, J.-P.; Roncin, J.; Misawa, H.; Sakuragi, H.; Tokumaru, K. *Bull. Chem. Soc. Jpn.* **1990**, *63*, 347.

(22) Maillard, B.; Ingold, K. U.; Scaiano, J. C. *J. Am. Chem. Soc.* **1983**, *105*, 5095.

JP9609904